



Pre- and Post-treatment Double-Sequential-Point Dynamic Radiomic Model in the Response Prediction of Gastric Cancer to Neoadjuvant Chemotherapy: 3-Year Survival Analysis

Yinkui Wang, MD¹, Lei Tang, MD², Xiangji Ying, MPH, MS³, Jiazheng Li, MD², Fei Shan, MD¹, Shuangxi Li, MD¹, Yongning Jia, MD¹, Kan Xue, MD¹, Rulin Miao, MD¹, Zhemin Li, MD¹, Ziyu Li, MD¹, and Jiafu Ji, MD, PhD, DrPH¹ 

¹Gastrointestinal Cancer Center, Key Laboratory of Carcinogenesis and Translational Research (Ministry of Education), Peking University Cancer Hospital & Institute, Hai-Dian District, Beijing, People's Republic of China; ²Department of Radiology, Key Laboratory of Carcinogenesis and Translational Research (Ministry of Education), Peking University Cancer Hospital and Institute, Beijing, People's Republic of China; ³Department of Epidemiology, Johns Hopkins Bloomberg School of Public Health, Baltimore, MD

ABSTRACT

Background. Prognosis prediction of patients with gastric cancer after neoadjuvant chemotherapy is suboptimal. This study aims to develop and validate a dynamic radiomic model for prognosis prediction of patients with gastric cancer on the basis of baseline and posttreatment features.

Patients and methods. This single-center cohort study included patients with gastric adenocarcinoma treated with neoadjuvant chemotherapy from June 2009 to July 2015 in the Gastrointestinal Cancer Center of Peking University Cancer Hospital. Their clinicopathological data, pre-treatment and post-treatment computed tomography (CT) images, and pathological reports were retrieved and analyzed. Four prediction models were developed and validated using tenfold cross-validation, with death within 3 years as the outcome. Model discrimination was compared by the area under the curve (AUC). The final radiomic model was

evaluated for calibration and clinical utility using Hosmer–Lemeshow tests and decision curve analysis.

Results. The study included 205 patients with gastric adenocarcinoma [166 (81%) male; mean age 59.9 (SD 10.3) years], with 71 (34.6%) deaths occurring within 3 years. The radiomic model alone demonstrated better discrimination than the pathological T stage (ypT) stage model alone (cross-validated AUC 0.598 versus 0.516, $P = 0.009$). The final radiomic model, which incorporated both radiomic and clinicopathological characteristics, had a significantly higher cross-validated AUC (0.769) than the ypT stage model (0.516), the radiomics alone model (0.598), and the ypT plus other clinicopathological characteristics model (0.738; all $P < 0.05$). Decision curve analysis confirmed the clinical utility of the final radiomic model.

Conclusions. The developed radiomic model had good accuracy and could be used as a decision aid tool in clinical practice to differentiate prognosis of patients with gastric cancer.

Yinkui Wang, Lei Tang, Xiangji Ying and Jiazheng Li are shared first author.

© Society of Surgical Oncology 2023

First Received: 3 January 2023

Accepted: 9 October 2023

Published online: 22 November 2023

Z. Li, MD
e-mail: ziyu_li@hsc.pku.edu.cn

J. Ji, MD, PhD, DrPH
e-mail: jijiafu@hsc.pku.edu.cn

Keywords Gastric cancer · Neoadjuvant chemotherapy · Radiomics · Prediction model · Prognosis

Gastric cancer is the third leading cause of cancer-related deaths worldwide.¹ Neoadjuvant chemotherapy is increasingly used in clinical practice and has many advantages, such as increasing patient tolerance to chemotherapy, reducing potential micrometastasis, and increasing the rate of radical surgery. Previous phase III clinical trials have preliminarily

confirmed that perioperative chemotherapy combined with radical surgery can significantly improve the patient's prognosis.² The perioperative treatment modality of neoadjuvant chemotherapy combined with radical surgery has been recommended as a standard option by the clinical guidelines (evidence level 1, NCCN Guidelines 2021v4).³ Meanwhile, neoadjuvant chemotherapy is an *in vivo* drug sensitivity test that can help assess drug efficacy by evaluating tumor changes during chemotherapy and provide a basis for precise treatment of patients.

At present, imaging evaluation in gastric cancer mainly adopts the World Health Organization (WHO) efficacy evaluation criteria or Response Evaluation Criteria in Solid Tumors (RECIST).⁴ However, because the stomach is a hollow organ, the thickness of the stomach wall is affected by the degree of gastric cavity filling, and the staging of the primary lesion of the stomach is based on the depth of tumor invasion rather than the size of the tumor. Therefore, it is different from solid tumors such as those found in breast cancer and liver cancer. There are still many difficulties in evaluating the effect of neoadjuvant chemotherapy on gastric cancer. The primary lesion cannot be used as an evaluable lesion. If there is no obvious enlarged lymph node, it is difficult to accurately evaluate the response according to the existing standards. In some patients, although the size of the lesion does not change significantly during chemotherapy, the tumor cell density may have changed, so the change in diameter alone cannot reflect the tumor response. It has been reported in the literature that only 17% of patients with gastric cancer receiving neoadjuvant chemotherapy have a pathological tumor regression grade (TRG) of 1.⁵ This means that limited by the low accuracy of the response evaluation, a large number of patients who receive neoadjuvant chemotherapy for gastric cancer have received excessive chemotherapy, missed the optimal time for surgery, and suffered from reduced survival time.

A major focus and challenge in gastric cancer is how to effectively evaluate the efficacy of neoadjuvant chemotherapy. With the widespread application of artificial intelligence and deep learning in medicine,⁶ it has become possible to use radiomics to provide more valuable clinical information. The results of an earlier study conducted in our center suggest that radiomics can help identify occult peritoneal metastases.⁷ In recent years, there have also been studies suggesting that radiomics can predict patients' pathological stage or TRG.^{8,9} However, two research gaps remain. First, the pathological staging of ypT after chemotherapy alone or the TRG alone represents only part of the information about the effectiveness of chemotherapy in patients. Moreover, although Becker's¹⁰ study reported that the TRG is correlated with the pathological T stage after neoadjuvant chemotherapy, these two are not always linearly correlated. In the study of Katjia Ott et al.,¹¹ ypT3 and ypT4 patients

were as high as 40% among the 231 patients with residual tumor cells < 10%, while in patients with nonprimary lesion pCR with residual tumor cells less than 10%, ypT3 and ypT4 patients were as high as 54.3%. Second, the existing studies are primarily based on pre-treatment radiomics, while the changes in pre-treatment and post-treatment radiomics may better reflect the changes in the tumor during treatment and may be more representative of the patient's therapeutic effect.

Therefore, we conducted this retrospective single-center cohort study to explore whether baseline and post-treatment radiomic signatures can better predict prognosis of patients with gastric cancer.

PATIENTS AND METHODS

Patients

The study population included patients diagnosed with gastric adenocarcinoma by gastroscopic pathology from June 2009 to July 2015 at the Gastrointestinal Cancer Center of Peking University Cancer Hospital. Patients were included in the analyses if they met the following criteria: (a) confirmed gastric adenocarcinoma by gastroscopic pathology; (b) underwent preoperative staging of a locally advanced stage without distant metastasis; (c) received neoadjuvant chemotherapy based on platinum combined with fluorouracil regimen; (d) received baseline CT scan within 10 days before the initiation of the first cycle of chemotherapy and presurgery CT scan within 1 month after the completion of the last cycle of chemotherapy; (e) underwent radical distal gastrectomy or total gastrectomy with R0 resection; and (f) had regular follow-up in our hospital and complete clinical pathological data. Patients were excluded if they (a) died during the perioperative period; (b) received chemotherapy for other tumors within half a year before the diagnosis; (c) received preoperative neoadjuvant radiotherapy, targeted therapy, or immunotherapy; (d) had gastric remnant cancer; (e) received preventive intraperitoneal infusion chemotherapy; or (f) had poor CT image quality. The current study was approved by the Institutional Review Committee of Peking University Cancer Hospital (2019YJZ26).

CT Image Acquisition

All patients underwent enhanced CT examination of the abdomen and pelvis after fasting for more than 6–8 h. Before CT examination, 10 mg anisodamine (654-2, Hangzhou Minsheng Pharma) were injected intramuscularly, and 6 g gas-producing crystals with 10 ml warm water were administered orally to distend the gastric wall. The CT scan was performed either by the LightSpeed 64 VCT or the Discovery CT750 HD.

Tumor Segmentation

Baseline and presurgery enhanced CT in the arterial and venous phases were reviewed by two radiologists on ITK-SNAP (v.3.6.0, <http://www.itksnap.org>). The most evident part of the primary lesion on axial CT was manually delineated by one radiologist (doctor A with 15 years of experience in radiology) and supervised by a senior radiologist (doctor B with 20 years of experience in gastrointestinal radiology). Both radiologists were blinded to all patients' clinicopathological information but knew the location of gastric cancer according to endoscope results.

Measurements

The following clinical and pathological characteristics were collected: age, sex, comorbidity status, height, weight, Eastern Cooperative Oncology Group (ECOG) score, American Society of Anesthesiologists (ASA) score, number of preoperative chemotherapy cycles, preoperative chemotherapy regimen, operation duration, intraoperative blood loss, surgical approach, tumor location, tumor pathological type, degree of differentiation, pathological T stage (ypT), pathological N stage (ypN), vascular tumor thrombus, number of dissected lymph nodes, number of metastatic lymph nodes, and time between the completion of neoadjuvant chemotherapy and surgery.

Overall survival (OS) was defined as the time from diagnosis to death due to any reason or the last follow-up. On the basis of OS, we constructed a new outcome of death within 3 years, with 1 indicating that the patient died due to any cause within 3 years from the time of diagnosis.

Radiomic Feature Extraction

Image preprocessing was applied before feature extraction. For each patient, 408 radiomic features and 4 handcrafted features were extracted from the masked lesion area (Supplementary Figure S1). Radiomic features were calculated using the standardized algorithm available in pyradiomics. This encompasses first-order statistics that describe individual voxel values' distribution, shape-based features detailing the region of interest's shape, and texture features that elucidate voxel patterns and relationships, including the gray level co-occurrence matrix (GLCM), gray level run length matrix (GLRLM), gray level size zone matrix (GLSZM), neighboring gray tone difference matrix (NGTDM), and gray level dependence matrix (GLDM). Four handcrafted features were computed on the basis of the

skeleton of the lesion mask, all of which aimed to measure the length of the lesion.

Radiomic Feature Building

We applied Yeo-Johnson power transformation to normalize radiomic features. After transformation, the intra-class correlation coefficient (ICC) was utilized to evaluate the reproducibility and robustness of the extracted features. We applied perturbations to the lesion mask to construct multiple raters on the same feature, and features with $ICC < 0.8$ were excluded. Less than half of the radiomic features (185/408) had reproducibility and robustness ($ICC > 0.8$) under mask perturbation. To further eliminate redundant features, we applied consensus clustering with Pearson's correlation coefficient as the distance metric to group the features into clusters, and 12 features with the highest average consensus index in each cluster were selected (Supplementary Figure S2). These features were then divided into two groups. One group consisted of the radiomic features after neoadjuvant chemotherapy and therefore contained information on treatment results. The other group consisted of radiomic features of the before-and-after-chemotherapy difference and therefore contained information on treatment sensitivity. An overall radiomic score was built for each group of features by Cox regression with OS as the outcome.

Model Development and Validation

Associations of the radiomic signatures and clinical characteristics with death within 3 years were examined by univariable logistic regression. Variables were selected into the prediction models on the basis of their contributions to the prediction accuracy. We built four models: one model with ypT stage only (T model), one model with only radiomic features (RS model), one model with ypT stage and clinical characteristics (T+ model), and one model with radiomic features (same as the RS model) and clinical characteristics (same as the T+ model but excluding the ypT stage). The clinical characteristics included in the latter two models were histological grade, tumor location, vessel carcinoma embolus, and ypN stage.

We used tenfold cross-validation to validate the model performance. We assessed and compared the model accuracy using the AUC statistic. Model calibration was assessed by calibration plots and Hosmer–Lemeshow tests. Decision curve analysis was conducted to evaluate the models' clinical usefulness by quantifying the net benefit at different threshold probabilities.

Statistical analysis was conducted with STATA software (version 16) and R (version 4.2.1). A two-sided P -value < 0.05 was used to indicate statistical significance.

RESULTS

Patient Characteristics

The entire study cohort comprised 205 patients with gastric adenocarcinoma, with 71 (34.6%) deaths within 3 years (Table 1). Approximately 81% ($n = 166$) of the cohort was male, and the mean age was 59.9 (SD 10.3). Patients with adenocarcinoma made up 80.0% ($n = 164$) of the study

population. Most participants were at ypN 0 stage ($n = 81$, 39.5%) or at ypT 4 stage ($n = 105$, 51.2%).

Univariable Analyses

Univariable analyses showed that several patient characteristics were associated with death within 3 years, including BMI, degree of differentiation, tumor location, vessel carcinoma embolus, pathological short diameter, pathological long diameter, ypN stage, and ypT stage (all $P < 0.05$) (Table 1).

Seven candidate radiomic features were used for selection into the final models, of which three were significantly

TABLE 1 Association of patient clinicopathological characteristics with death within 3 years.

| Characteristic | Total ($N = 205$) | Events ($N = 71$) | Nonevents ($N = 134$) | P value |
|---|---------------------|---------------------|-------------------------|-----------|
| Sex | | | | |
| Male | 166 (81.0) | 57 (80.3) | 109 (81.3) | 0.85 |
| Female | 39 (19.0) | 14 (19.7) | 25 (18.7) | |
| Age, mean (\pm SD) | 59.9 \pm 10.3 | 59.7 \pm 11.4 | 60.0 \pm 9.7 | 0.80 |
| BMI, mean (\pm SD) | 24.3 \pm 3.5 | 23.6 \pm 3.2 | 24.7 \pm 3.6 | 0.040 |
| Degree of differentiation | | | | |
| Well/moderate/moderate to well | 57 (27.8) | 11 (15.5) | 46 (34.3) | 0.009 |
| Moderate to poor | 53 (25.9) | 24 (33.8) | 29 (21.6) | |
| Poor | 95 (46.3) | 36 (50.7) | 59 (44.0) | |
| Pathological type | | | | |
| Adenocarcinoma | 164 (80.0) | 52 (73.2) | 112 (83.6) | 0.081 |
| Others | 41 (20.0) | 19 (26.8) | 22 (16.4) | |
| Tumor location | | | | |
| Upper | 76 (37.1) | 18 (25.4) | 58 (43.3) | 0.002 |
| Middle | 24 (11.7) | 11 (15.5) | 13 (9.7) | |
| Lower | 90 (43.9) | 31 (43.7) | 59 (44.0) | |
| Total | 15 (7.3) | 11 (15.5) | 4 (3.0) | |
| Vessel carcinoma embolus | | | | |
| No | 113 (55.1) | 24 (33.8) | 89 (66.4) | < 0.001 |
| Yes | 74 (36.1) | 42 (59.2) | 32 (23.9) | |
| Unclear | 18 (8.8) | 5 (7.0) | 13 (9.7) | |
| Pathological short diameter, mean (\pm SD) | 3.1 \pm 2.7 | 3.8 \pm 3.2 | 2.7 \pm 2.3 | 0.007 |
| Pathological long diameter, mean (\pm SD) | 4.5 \pm 3.2 | 5.6 \pm 3.6 | 3.9 \pm 2.9 | < 0.001 |
| ypN | | | | |
| 0 | 81 (39.5) | 9 (12.7) | 72 (53.7) | < 0.001 |
| 1 | 36 (17.6) | 14 (19.7) | 22 (16.4) | |
| 2 | 38 (18.5) | 13 (18.3) | 25 (18.7) | |
| 3a | 25 (12.2) | 15 (21.1) | 10 (7.5) | |
| 3b | 25 (12.2) | 20 (28.2) | 5 (3.7) | |
| ypT | | | | |
| 1–2 | 54 (26.3) | 10 (14.1) | 44 (32.8) | 0.011 |
| 3 | 46 (22.4) | 19 (26.8) | 27 (20.1) | |
| 4 | 105 (51.2) | 42 (59.2) | 63 (47.0) | |

Numbers are displayed as n (column percentage) unless otherwise specified

P values are derived by univariable logistic regression of death within 3 years on each variable

TABLE 2 Association of candidate radiomic features with death within 3 years.

| Radiomic feature | Mean (\pm SD) | <i>P</i> -value ¹ | Non-CV AUC (95% CI) | <i>P</i> -value ² | CV AUC (95% CI) | <i>P</i> value ³ |
|-------------------------|---------------------|------------------------------|---------------------|------------------------------|---------------------|-----------------------------|
| Score_after | 1.134 \pm 0.412 | 0.004 | 0.638 (0.560–0.715) | 0.45 | 0.634 (0.531–0.686) | 0.004 |
| Score_diff | 1.033 \pm 0.313 | 0.118 | 0.570 (0.489–0.651) | 0.62 | 0.576 (0.450–0.612) | 0.19 |
| After_SmallAreaEmphasis | 0.481 \pm 0.093 | 0.101 | 0.555 (0.475–0.635) | 0.43 | 0.562 (0.444–0.605) | 0.22 |
| After_Sphericity | 0.557 \pm 0.143 | 0.004 | 0.622 (0.542–0.701) | 0.66 | 0.616 (0.534–0.698) | 0.010 |
| Diff_RunEntropy | –0.097 \pm 0.347 | 0.090 | 0.549 (0.468–0.630) | 0.35 | 0.534 (0.434–0.594) | 0.26 |
| Diff_InverseVariance | 0.009 \pm 0.056 | 0.20 | 0.548 (0.466–0.631) | 0.41 | 0.539 (0.453–0.620) | 0.33 |
| After_long | 72.755 \pm 52.531 | 0.011 | 0.679 (0.606–0.752) | 0.10 | 0.670 (0.566–0.721) | < 0.001 |

CV cross-validation, *score_after* radiomic signature constructed based on postchemotherapy features, *score_diff* radiomic signature constructed on the basis of the difference in postchemotherapy features, *after_SmallAreaEmphasis* small area emphasis of the postchemotherapy arterial phase GLSZM matrix, *after_Sphericity* shape2D sphericity of the postchemotherapy venous phase, *diff_RunEntropy* difference in pre- and postchemotherapy arterial phase GLRLM matrix run entropy, *diff_InverseVariance* difference in pre- and postchemotherapy arterial phase GLCM matrix inverse variance, *after_long* long diameter of postchemotherapy arterial phase lesion

¹*P* values are derived by univariable logistic regression of death within 3 years on each radiomic feature

²*P* values are derived by comparing the noncross-validated AUC of the radiomic feature to the noncross-validated AUC of the ypT stage

³*P* values are derived by comparing the cross-validated AUC of the radiomic feature to the cross-validated AUC of the ypT stage

associated with death within 3 years (Table 2). After cross-validation, three radiomic features (*score_after*, *after_Sphericity*, *after_long*) had an AUC value that was significantly higher than that of ypT stage (all *P* < 0.05). The individual cross-validated AUC statistic ranged from 0.534 to 0.670.

Model Performance

Table 3 presents the models' AUC values. The non-cross-validated AUCs were 0.597 (95% CI 0.525–0.669), 0.654 (95% CI 0.579–0.729), 0.823 (95% CI 0.760–0.885), and 0.833 (95% CI 0.777–0.890) for the T, RS, T+, and RS+ models, respectively. The cross-validated AUC of the RS model was significantly higher than that of the T model (0.598 versus 0.516, *P* = 0.009). The cross-validated AUC of the RS+ model was significantly higher than that of the T model (0.769 versus 0.516, *P* < 0.001), the RS model (0.769

versus 0.598, *P* < 0.001), and the T+ model (0.769 versus 0.738, *P* = 0.023).

The calibration plot (Figure 1A) and Hosmer–Lemeshow test (*P* = 0.92) indicated that the RS+ model performed well in terms of calibration when not subjected to cross-validation. After cross-validation, the calibration plot (Figure 1B) revealed a discrepancy between the observed and expected outcomes. The Hosmer–Lemeshow test was statistically significant (*P* = 0.026), indicating a departure from the ideal fit between the predicted and observed outcomes. In the decision curve plot (Figure 2), the T+ and RS+ models had comparable net benefits greater than the T and RS models at all threshold probabilities.

DISCUSSION

In the current study, we built a radiomic model predicting prognosis of patients with gastric cancer after

TABLE 3 Model AUCs and their comparisons

| Models | AUC (95% CI) | | | | <i>P</i> value | | | |
|---------------------|---------------------|---------------------|---------------------|---------------------|----------------|---------------|---------------|--------------|
| | T | RS | T+ | RS+ | RS versus T | RS+ versus T+ | RS+ versus RS | RS+ versus T |
| Non-cross-validated | 0.597 (0.525–0.669) | 0.654 (0.579–0.729) | 0.823 (0.760–0.885) | 0.833 (0.777–0.890) | 0.27 | 0.43 | < 0.001 | < 0.001 |
| Cross-validated | 0.516 (0.358–0.520) | 0.598 (0.518–0.673) | 0.738 (0.645–0.795) | 0.769 (0.685–0.825) | 0.009 | 0.023 | < 0.001 | < 0.001 |

Model T: ypT stage

Model RS: radiomic signature (*score_after*, *score_diff*, *after_SmallAreaEmphasis*, *after_Sphericity*, *afeter_long*)

Model T+: ypT stage + other clinical characteristics (histological grade, tumor location, vessel carcinoma embolus, ypN stage)

Model RS+: radiomic signature (same as the RS model) + other clinical characteristics (histological grade, tumor location, vessel carcinoma embolus, ypN stage)

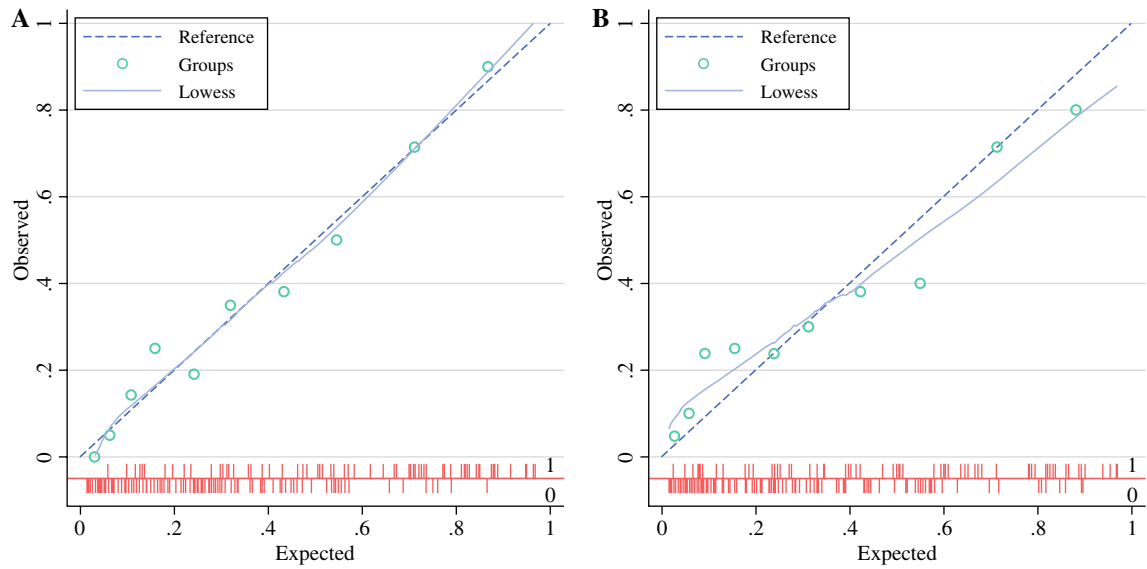


FIG. 1 Calibration curves of the RS+ model in the development cohort (A) and after cross-validation (B).

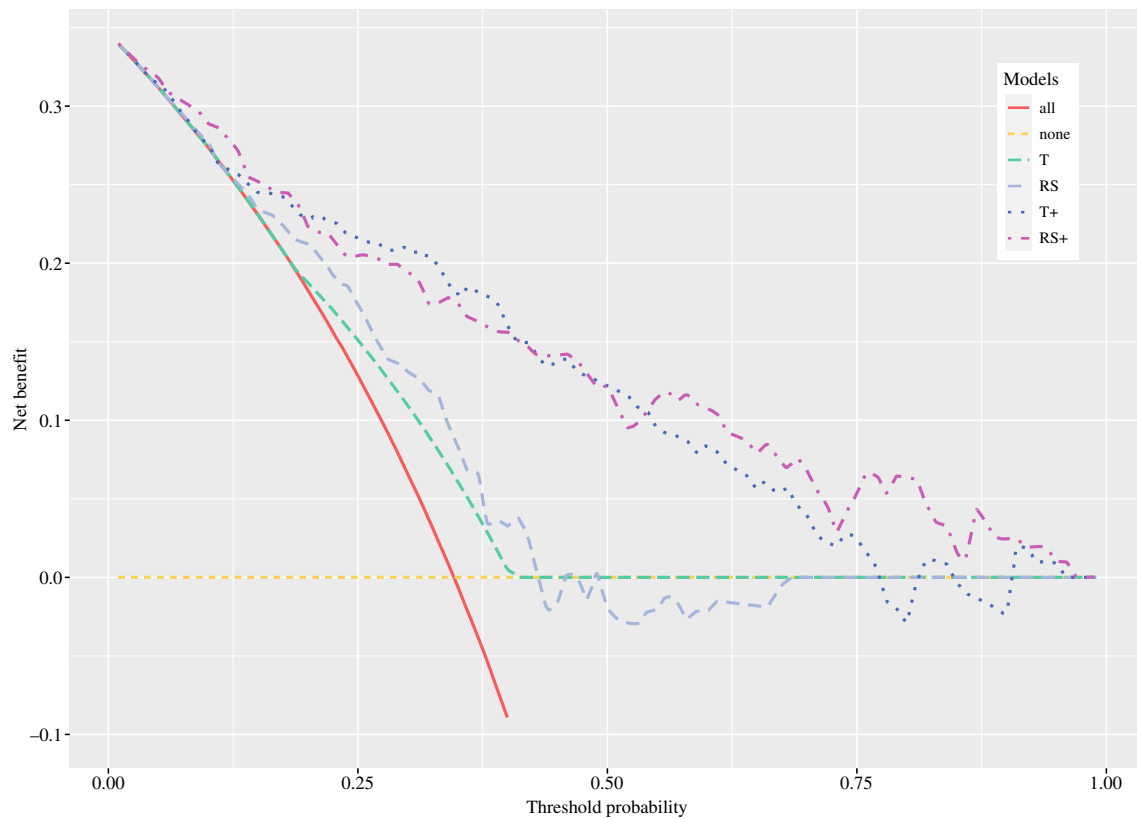


FIG. 2 Decision curve analysis for all models.

neoadjuvant chemotherapy. The final model included both pre-treatment and post-treatment radiomic signatures, along with clinicopathological characteristics. The model demonstrated excellent prediction accuracy in the

development set, and its accuracy remained acceptable after cross-validation.

Unlike those who only undergo surgery, patients with neoadjuvant chemotherapy have more influencing factors

on prognosis, including the patient's baseline tumor stage, response to chemotherapy, surgical radicality, and so on. Therefore, it is relatively more difficult to evaluate the prognosis of patients with gastric cancer after neoadjuvant chemotherapy. From the perspective of pathological staging alone, for patients undergoing direct surgery, the currently reported AUC of pTNM staging was 0.719,¹² while the AUC of ypTNM staging in patients after neoadjuvant chemotherapy was 0.657,¹³ indicating the difficulty of prognostic evaluation of patients after neoadjuvant chemotherapy, and the existing standards are far from meeting the clinical needs. Past research on gastric cancer radiomics has mainly focused on the prediction of peritoneal metastasis, lymph node metastasis, and pathological staging. In terms of prognosis, the only available study suggested that the AUC was 0.860 in the training set for a model consisting of radiomic and clinicopathological characteristics.¹⁴ For the efficacy of neoadjuvant chemotherapy, previous studies have used pre-treatment radiomics to predict patient TRG, with an AUC of 0.736 in the training set and 0.679 in the validation set.⁸ There are also studies predicting pathological ypT0–1 stage through baseline radiomics and clinicopathological characteristics. The AUC was 0.763 in the training set and 0.744 in the validation set.⁹ A study predicting tumor downstaging with baseline or after treatment CT scans yielded an AUC between 0.750 and 0.966.¹⁵ Our study first used radiomics and clinicopathological information to predict the survival of patients after neoadjuvant chemotherapy and reached AUCs comparable to those of previous studies (0.769–0.833).

The prognosis of patients after neoadjuvant chemotherapy depends on two aspects: the pathological stage of the patient before chemotherapy and the tumor's response to chemotherapy. In the current analysis, we included the radiomic information of patients at baseline and after chemotherapy. We also achieved delineation and calculation of the tumor long diameter through radiomic artificial intelligence. On the basis of the cross-validation results, it was found that three radiomic features, namely *score_after*, *after_Sphericity*, and *after_long*, had significantly higher AUC values than the ypT stage. The *score_after* variable represents the radiomic signature constructed using post-chemotherapy features. The *after_Sphericity* variable provides information on the 2D shape sphericity of the post-chemotherapy primary lesion. Finally, our *after_long* indicator measures the size of irregular lesions through radiomics.

In addition to the acceptable to excellent prediction accuracy of the RS+ model, another important clinical implication of the current study is that it provides a new approach for evaluating chemotherapy efficacy for patients with gastric cancer undergoing neoadjuvant chemotherapy. At present, the RECIST standard is used to evaluate the effect of neoadjuvant chemotherapy for gastric cancer in clinical practice and is also regarded as the gold standard for solid tumors.¹⁶

However, its application in gastric cancer has limitations. The stomach is a hollow organ, and its primary lesion cannot be evaluated as a target lesion. Studies have suggested that the evaluation result of RECIST was not an independent prognostic factor for patients with gastric cancer after neoadjuvant chemotherapy.^{17,18} Four of the radiomic features in the current study were independently associated with patient prognosis. It may provide a more accurate evaluation of neoadjuvant chemotherapy efficacy for patients with gastric cancer. For patients with a good predicted prognosis, surgery may be considered, while for patients with a poor predicted prognosis, it may be more appropriate to consider extending the number of chemotherapy cycles or adjusting the chemotherapy regimen to achieve more precise treatment of the patient. At the same time, the limitation of the lack of target lesions in the RECIST standard was avoided because the region of interest (ROI) of the radiomics mainly focused on the primary lesion.

Our study has several limitations. A major one is the choice of ROI. We chose the CT image of the most evident part of the tumor for delineation and did not delineate the lesion layer by layer. Because of the heterogeneity of gastric cancer, layer-by-layer delineation might improve the prediction accuracy of the model but also reduce the feasibility of radiomics, as it requires manual delineation. The ROI delineated only the primary tumor and did not involve the lymph nodes. However, we did not delineate the lymph node area for two reasons. On the one hand, clinical imaging has limited accuracy in judging whether there is lymph node metastasis, generally approximately 64–66%.^{19–21} Through the new technology of radiomics, the AUC of lymph node metastasis can be increased to 0.9319 in the training set and 0.8546 in the validation set. For patients after neoadjuvant chemotherapy, whether there is lymph node metastasis before chemotherapy cannot be pathologically verified, and lymph node metastasis after chemotherapy is more difficult to judge because of the chemotherapy. On the other hand, some studies have suggested that the imaging characteristics of the primary tumor could indicate whether the lymph node has metastasized.^{22–24}

Other limitations include the following. We used a retrospective dataset from a single center to develop the models, and the sample size was not very large. This may limit the generalizability of the results. Due to data availability and accuracy issues, we were unable to analyze important prognostic factors, such as clinical T stage before neoadjuvant chemotherapy and TRG. The use of the model requires researchers to manually delineate the ROI on the CT scan. To simplify the model, we dichotomized patient survival into alive or dead within 3 years, which caused some information on the length of survival time to be lost. The clinical meaning of some extracted radiomic features can be elusive and inexplicable. The associations of these features with patient

clinical manifestations should be further investigated. The AUCs of the RS+ model were high, but the calibration after cross-validation was poor. The model's robustness needs to be further validated in future research.

In summary, we developed and validated a pre- and post-treatment double-sequential-point dynamic radiomic prediction model on the basis of CT phenotypes and clinical characteristics for the prediction of prognosis among patients with gastric cancer after neoadjuvant chemotherapy. The model had good accuracy and could be used as a decision aid tool in clinical practice to differentiate patient prognosis.

SUPPLEMENTARY INFORMATION The online version contains supplementary material available at <https://doi.org/10.1245/s10434-023-14478-0>.

FUNDING This study is supported by the National Natural Science Foundation of China (31870805), Beijing Municipal Health Commission (DFL20181103), Beijing Natural Science Foundation (no. Z180001), PKU-Baidu Fund (no. 2020BD027), and Beijing Nova Program (20220484111).

DISCLOSURE

Conflicts of interest The authors declare that they have no conflicts of interest.

REFERENCES

- Chen W, Zheng R, Baade PD, Zhang S, Zeng H, Bray F, et al. Cancer statistics in China, 2015. *CA Cancer J Clin*. 2016;66(2):115–32.
- What is Quality of Care and why is it important? [Available from: http://www.who.int/maternal_child_adolescent/topics/quality-of-care/definition/en/].
- Jaffer A, Ajani M, Thomas A, D'Amico, MD, David J, Bentrem, MD, et al. NCCN Guidelines Version 4.2021. 2021.
- Grimaldi S, Terroir M, Caramella C. Advances in oncological treatment: limitations of RECIST 1.1 criteria. *Q J Nucl Med Mol Imaging* 2018;62(2):129–39.
- Blackham AU, Greenleaf E, Yamamoto M, Hollenbeak C, Gusani N, Coppola D, et al. Tumor regression grade in gastric cancer: predictors and impact on outcome. *J Surg Oncol*. 2016;114(4):434–9.
- Tschandl P, Codella N, Akay BN, Argenziano G, Braun RP, Cabo H, et al. Comparison of the accuracy of human readers versus machine-learning algorithms for pigmented skin lesion classification: an open, web-based, international, diagnostic study. *Lancet Oncol*. 2019;20(7):938–47.
- Dong D, Tang L, Li ZY, Fang MJ, Gao JB, Shan XH, et al. Development and validation of an individualized nomogram to identify occult peritoneal metastasis in patients with advanced gastric cancer. *Ann Oncol Off J Eur Soc Med Oncol*. 2019;30(3):431–8.
- Wang W, Peng Y, Feng X, Zhao Y, Seeruttun SR, Zhang J, et al. Development and validation of a computed tomography-based radiomics signature to predict response to neoadjuvant chemotherapy for locally advanced gastric cancer. *JAMA Netw Open*. 2021;4(8):e2121143.
- Chen Y, Wei K, Liu D, Xiang J, Wang G, Meng X, et al. A machine learning model for predicting a major response to neoadjuvant chemotherapy in advanced gastric cancer. *Front Oncol*. 2021;11:675458.
- Becker K, Langer R, Reim D, Novotny A, Meyer zum Buschenfelde C, Engel J, et al. Significance of histopathological tumor regression after neoadjuvant chemotherapy in gastric adenocarcinomas: a summary of 480 cases. *Ann Surg*. 2011;253(5):934–9.
- Ott K, Blank S, Becker K, Langer R, Weichert W, Roth W, et al. Factors predicting prognosis and recurrence in patients with esophago-gastric adenocarcinoma and histopathological response with less than 10% residual tumor. *Langenbeck's Arch Surg*. 2013;398(2):239–49.
- In H, Solsky I, Palis B, Langdon-Embry M, Ajani J, Sano T. Validation of the 8th edition of the AJCC TNM staging system for gastric cancer using the national cancer database. *Ann Surg Oncol*. 2017;24(12):3683–91.
- Li Z, Wang Y, Shan F, Ying X, Wu Z, Xue K, et al. ypTNM staging after neoadjuvant chemotherapy in the Chinese gastric cancer population: an evaluation on the prognostic value of the AJCC eighth edition cancer staging system. *Gastric Cancer*. 2018;21(6):977–87.
- Jiang Y, Chen C, Xie J, Wang W, Zha X, Lv W, et al. Radiomics signature of computed tomography imaging for prediction of survival and chemotherapeutic benefits in gastric cancer. *EBio-Medicine*. 2018;36:171–82.
- Xu Q, Sun Z, Li X, Ye C, Zhou C, Zhang L, et al. Advanced gastric cancer: CT radiomics prediction and early detection of downstaging with neoadjuvant chemotherapy. *Eur Radiol*. 2021;31(11):8765–74.
- Eisenhauer EA, Therasse P, Bogaerts J, Schwartz LH, Sargent D, Ford R, et al. New response evaluation criteria in solid tumors: revised RECIST guideline (version 1.1). *Eur J Cancer (Oxford, England: 1990)*. 2009;45(2):228–47.
- Xu X, Zheng G, Zhang T, Zhao Y, Zheng Z. Is pathologic tumor regression grade after neo-adjuvant chemotherapy a promising prognostic indicator for patients with locally advanced gastric cancer? A cohort study evaluating tumor regression response. *Cancer Chemother Pharmacol*. 2019;84(3):635–46.
- Kurokawa Y, Shibata T, Sasako M, Sano T, Tsuburaya A, Iwasaki Y, et al. Validity of response assessment criteria in neoadjuvant chemotherapy for gastric cancer (JCOG0507-A). *Gastric Cancer*. 2014;17(3):514–21.
- Seevaratnam R, Cardoso R, McGregor C, Lourenco L, Mahar A, Sutradhar R, et al. How useful is preoperative imaging for tumor, node, metastasis (TNM) staging of gastric cancer? *A Meta Anal Gastric Cancer*. 2012;15(Suppl 1):S3–18.
- Bando E, Makuuchi R, Irino T, Tanizawa Y, Kawamura T, Terashima M. Validation of the prognostic impact of the new tumor-node-metastasis clinical staging in patients with gastric cancer. *Gastric Cancer*. 2019;22(1):123–9.
- Cardoso R, Coburn N, Seevaratnam R, Sutradhar R, Lourenco LG, Mahar A, et al. A systematic review and meta-analysis of the utility of EUS for preoperative staging for gastric cancer. *Gastric Cancer*. 2012;15(Suppl 1):S19–26.
- Chai R, Ma H, Xu M, Arefan D, Cui X, Liu Y, et al. Differentiating axillary lymph node metastasis in invasive breast cancer patients: a comparison of radiomic signatures from multiparametric breast MR sequences. *J Magn Reson Imaging*. 2019;50(4):1125–32.
- Kan Y, Dong D, Zhang Y, Jiang W, Zhao N, Han L, et al. Radiomic signature as a predictive factor for lymph node metastasis in early-stage cervical cancer. *J Magn Reson Imaging*. 2019;49(1):304–10.

24. Li C, Zhang S, Zhang H, Pang L, Lam K, Hui C, et al. Using the K-nearest neighbor algorithm for the classification of lymph node metastasis in gastric cancer. *Comput Math Methods Med.* 2012;2012:876545.

Publisher's Note Springer Nature remains neutral with regard to jurisdictional claims in published maps and institutional affiliations.

Springer Nature or its licensor (e.g. a society or other partner) holds exclusive rights to this article under a publishing agreement with the author(s) or other rightsholder(s); author self-archiving of the accepted manuscript version of this article is solely governed by the terms of such publishing agreement and applicable law.